Faculty of Geosciences
Mantle Dynamics

Three-dimensional instantaneous dynamics modeling of present-day Aegean subduction

Anne Glerum[1] (A.C.Glerum@uu.nl), Wim Spakman[1,2], Douwe van Hinsbergen[1], Casper Pranger[3], Cedric Thieulot[1], Menno Fraters[1]

[1] Utrecht University, Department of Earth Sciences, Utrecht, The Netherlands
[2] University of Oslo, Centre of Earth Evolution and Dynamics (CEED), Oslo, Norway
[3] ETH Zurich, Institute of Geophysics, Zurich, Switzerland

Abstract

The Aegean region (eastern Mediterranean) has known continuous subduction for at least 100 My (van Hinsbergen et al., 2005), rendering it an ideal candidate for the study of the interaction between crustal tectonics, plate motion, subduction and mantle flow. To better understand this coupling of the tectonic evolution of the crust and the underlying mantle dynamics, we have developed 3D numerical models of the instantaneous dynamics of the present-day Aegean subduction system.

Model setup

We use the finite element code ASPECT (Kronbichler et al., 2012) and have developed additional plugins to create complex, realistic model set-ups (see **Fig. 1**). For example, the geometry of the subducting slab is inferred from seismic tomography (Amaru, 2007) and earthquake hypocenters (NCEDC, 2014), and the plate boundary configuration is based on those of Bird (2003) and the tectonic map of Faccenna et al. (2014). Crust and lithosphere thickness variations are abstracted from Moho and LAB maps (Faccenna et al., 2014, Carafa et al., 2015). The mantle initial temperature conditions can include variations to an adiabatic profile from conversion of seismic velocity anomalies (e.g. Steinberger and Calderwood, 2006).

Mantle flow at the model boundaries is either left free through open boundary conditions (Chertova et al., 2012) or is free slip. The bounding plate velocities are from Nocquet (2012) in the absolute Nubia frame of Doubrovine et al. (2012). A viscoplastic rheology is used for the plates and mantle ($\eta_{eff\ crust} \approx$ 1e24 Pas), while a constant viscosity is prescribed in the plate boundary faults. Material properties are taken from P,T lookup tables produced by Perple_X (Connolly, 2009).

Models

We have first tested the effect of different tomographic models (e.g. UU-P07 (Amaru, 2007) and TX2015 (Lu and Grand, 2016)) as well as methods for converting seismic velocity to temperature on model predictions of the regional flow field. Models shown here combine representative initial conditions with constructed variations in plate boundary strength, mantle temperature structure and boundary conditions.

Preliminary results

The free slip models in **Fig. 2 and 3** show Aegean plate motion driven by slab pull of the Hellenic (and Cyprus) slab. A first order match of model predictions of crustal velocity to GPS velocities is obtained with the models in **Fig. 4-6**, where plate velocities are prescribed on the lateral boundaries, although fine-tuning of fault rheology and boundary conditions is required.

Future work

Higher resolution runs will be performed on the Dutch Supercomputer, investigating the effect on surface deformation of varying mantle thermal structure, slab morphology and tearing, and absolute plate velocities. This way we will quantify the coupling of crust and mantle dynamics.

Table 1 Characteristics of models in **Figs. 2-6**.

	Fault rheology	Plate Boundary Conditions (BC)	Mantle BC	Tomo model
Fig. 2	1e21-1e22 Pas	Free slip	Free slip	-
Fig. 3	1e21-1e22 Pas	Free slip	Free slip	UU-P07
Fig. 4	1e20 Pas	Absolute plate motions, all sides	Open	UU-P07
Fig. 5	1e21 Pas	Absolute plate motions, all sides	Open	-
Fig. 6	1e20 Pas	Absolute plate motions, west open	Open	-

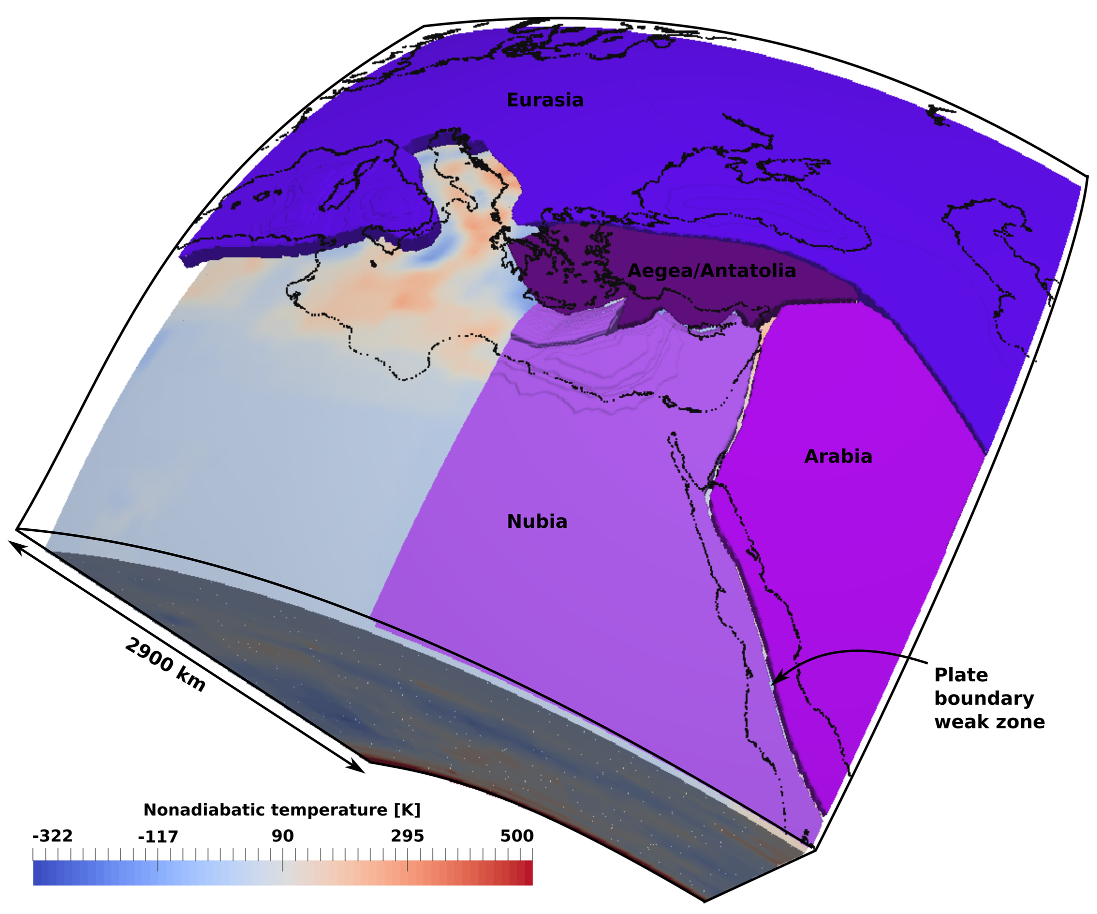

Figure 1 Example model setup: In purple colors the four plates with variable thickness and type (oceanic versus continental). The Nubian plate is partly removed to show the initial temperature conditions from 200 km depth to the core-mantle boundary. The lateral temperature variations are based on the tomographic model UU-P07 (Amaru, 2007). Plate boundary faults zones are 25 km wide.

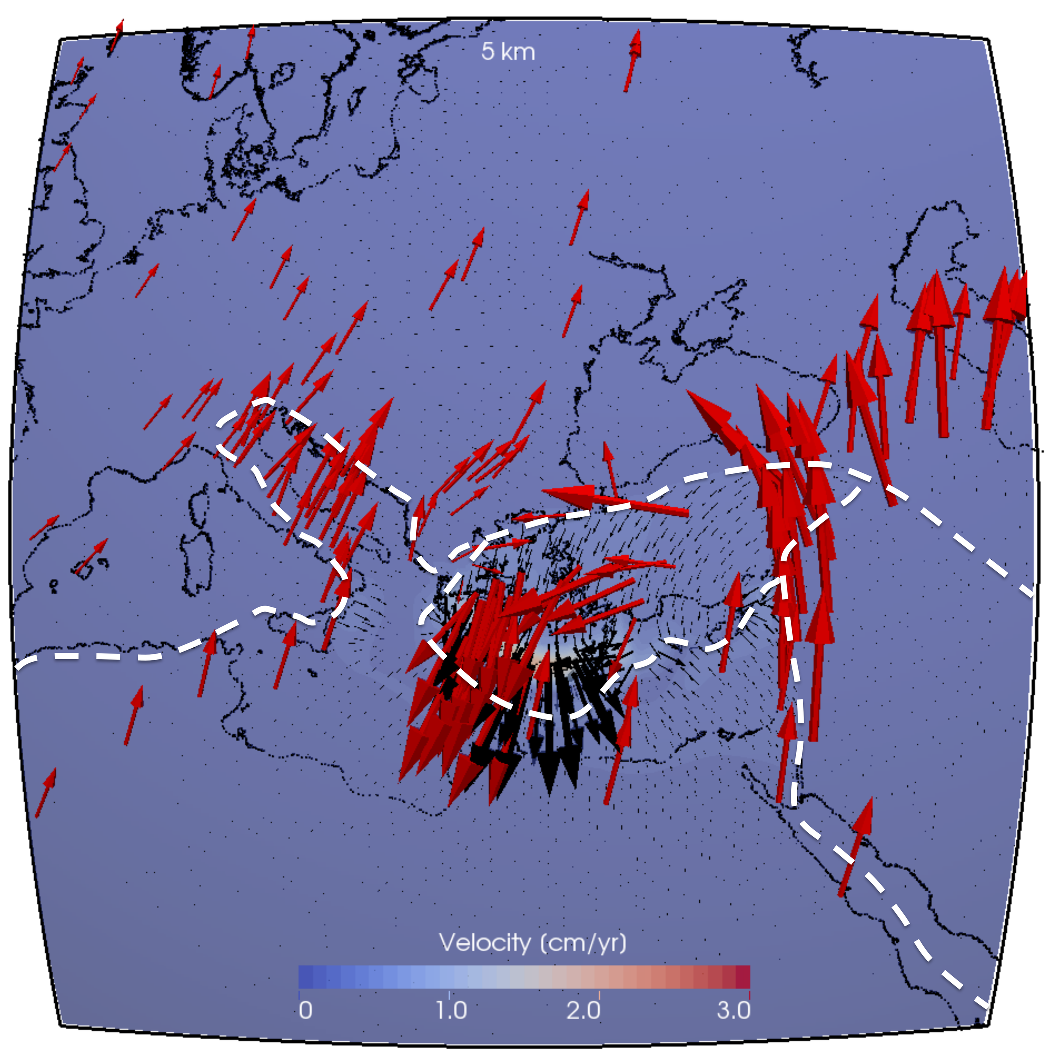

Figure 2 Lateral slice through model domain at 5 km depth showing the velocity magnitude field. Black vectors show the direction of velocity and can be compared to the GPS velocity vectors (in red) from Nocquet (2012) in the absolute plate motion frame of Doubrovine et al. (2012). White dashed lines show the approximate location of the model plate boundaries. Note that motion is concentrated in the Aegean plate, with a gradual increase in velocity towards the trench. GPS velocities do not match in magnitude, and little in direction.

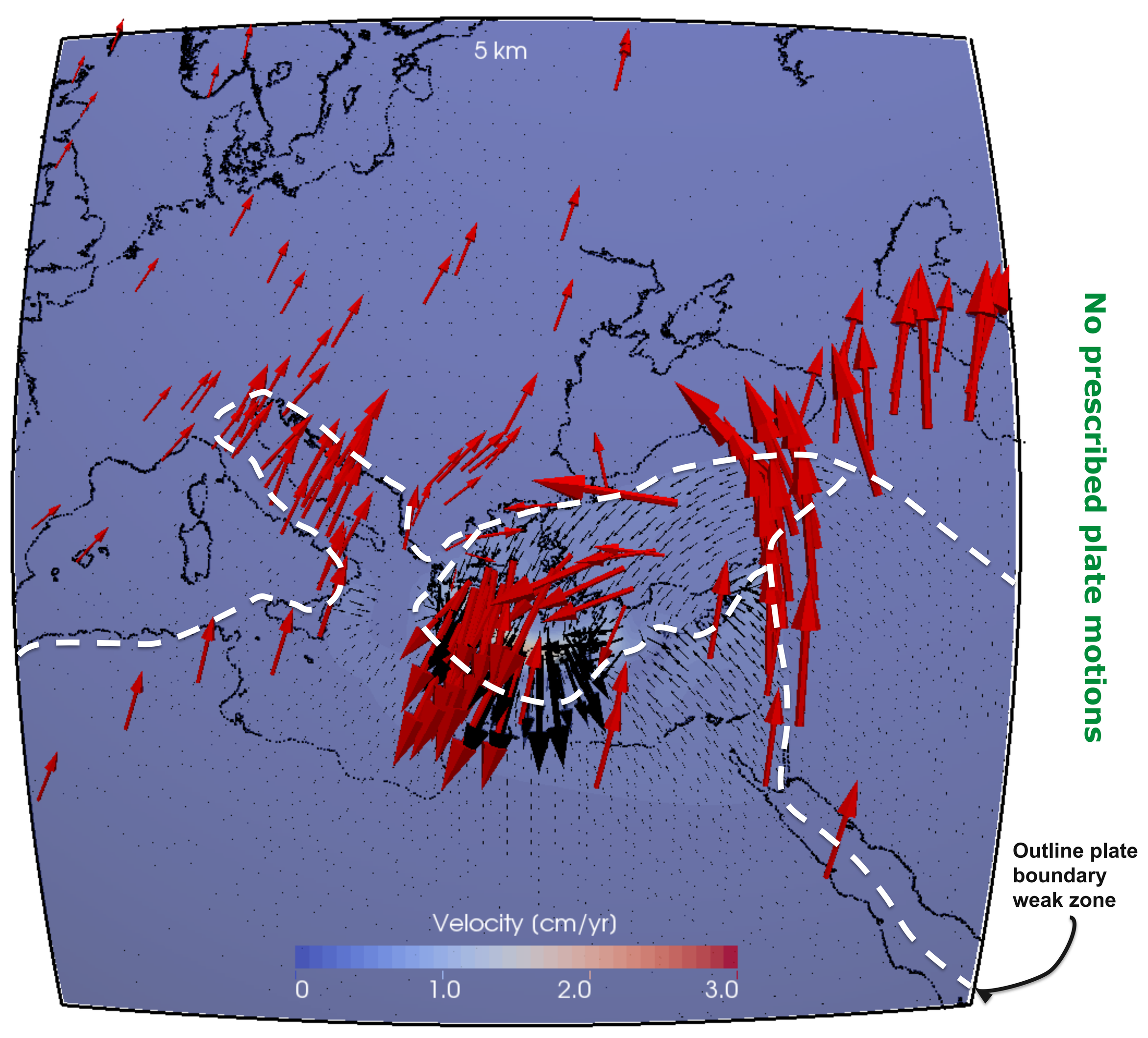

Figure 3 Adding lateral temperature variations in the mantle derived from tomographic model UU-P07 results in a more westward component of Aegean velocity in this free slip model.

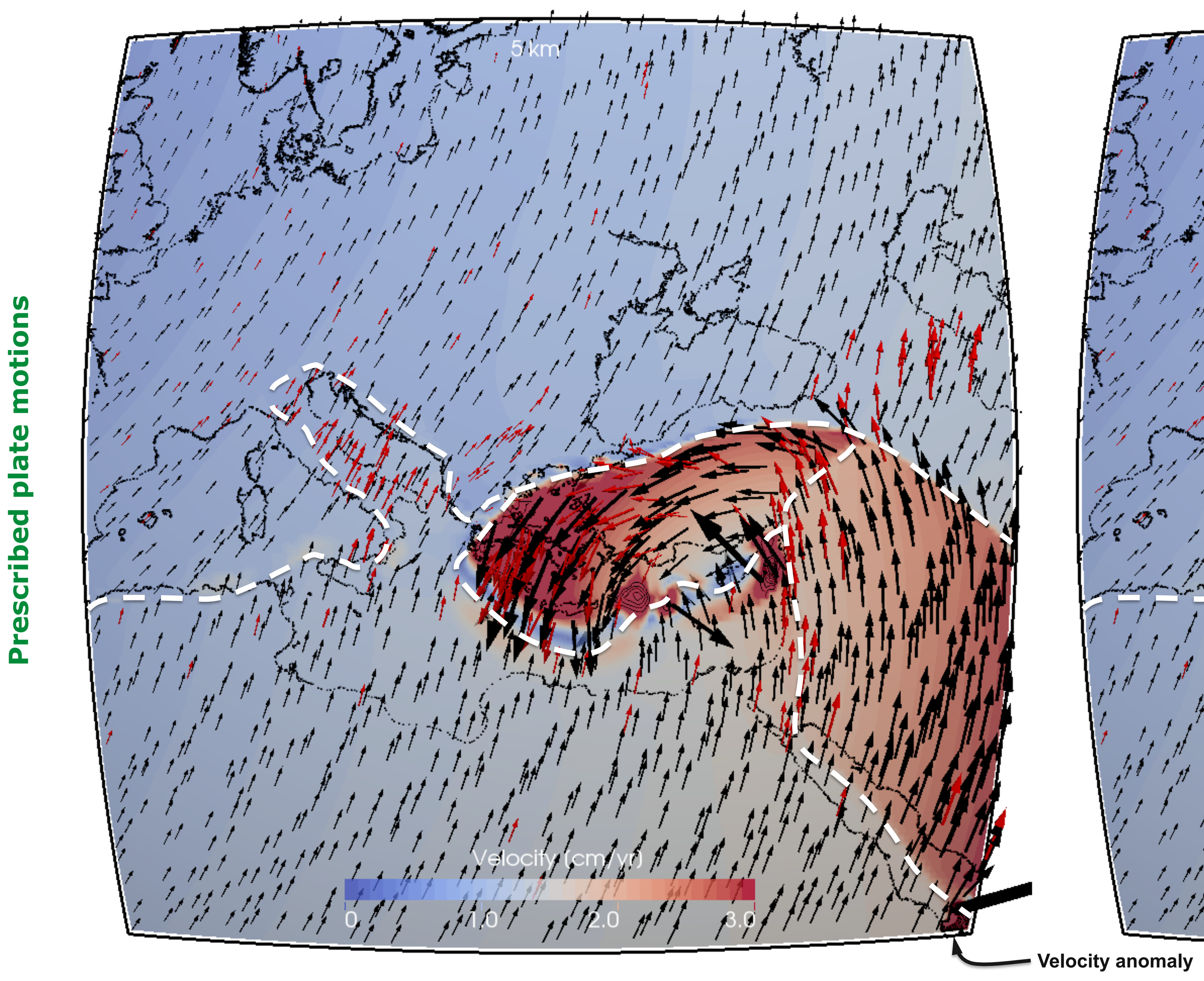

Figure 4 Prescribing the plate velocities on the upper 220 km of the lateral boundaries results in a first order match with the GPS velocities (red) in both magnitude and direction. Within the Aegaen plate, velocity increase is more gradual than in **Fig. 2 and 3**, but Anatolia motion is too trench-directed. NB: Velocity vector scale factor is 3 times smaller than in **Fig. 2 and 3**.

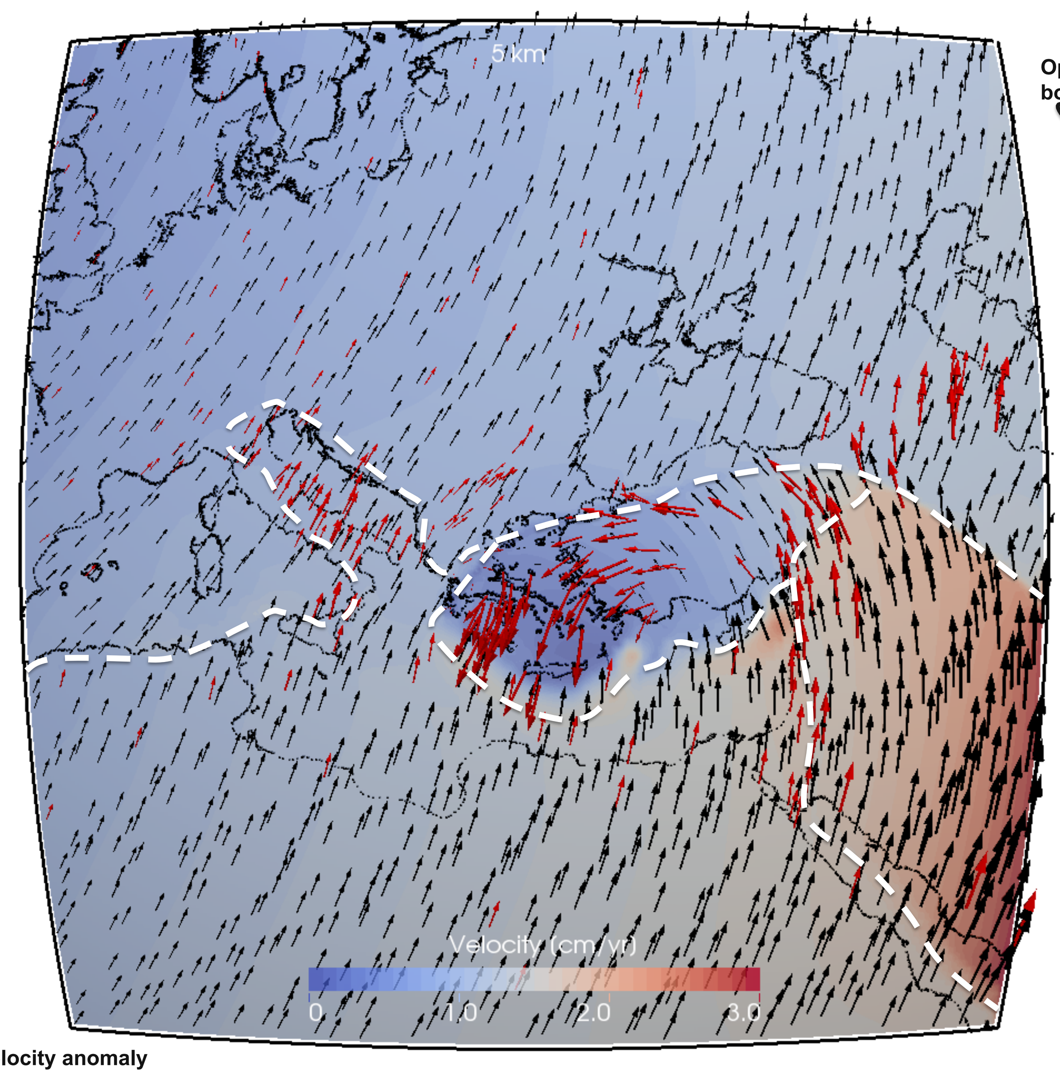

Figure 5 A higher constant viscosity of the plate boundaries increases coupling between the plates, leading to less slab rollback and a significant northward component of Aegaen motion transferred from Arabia.

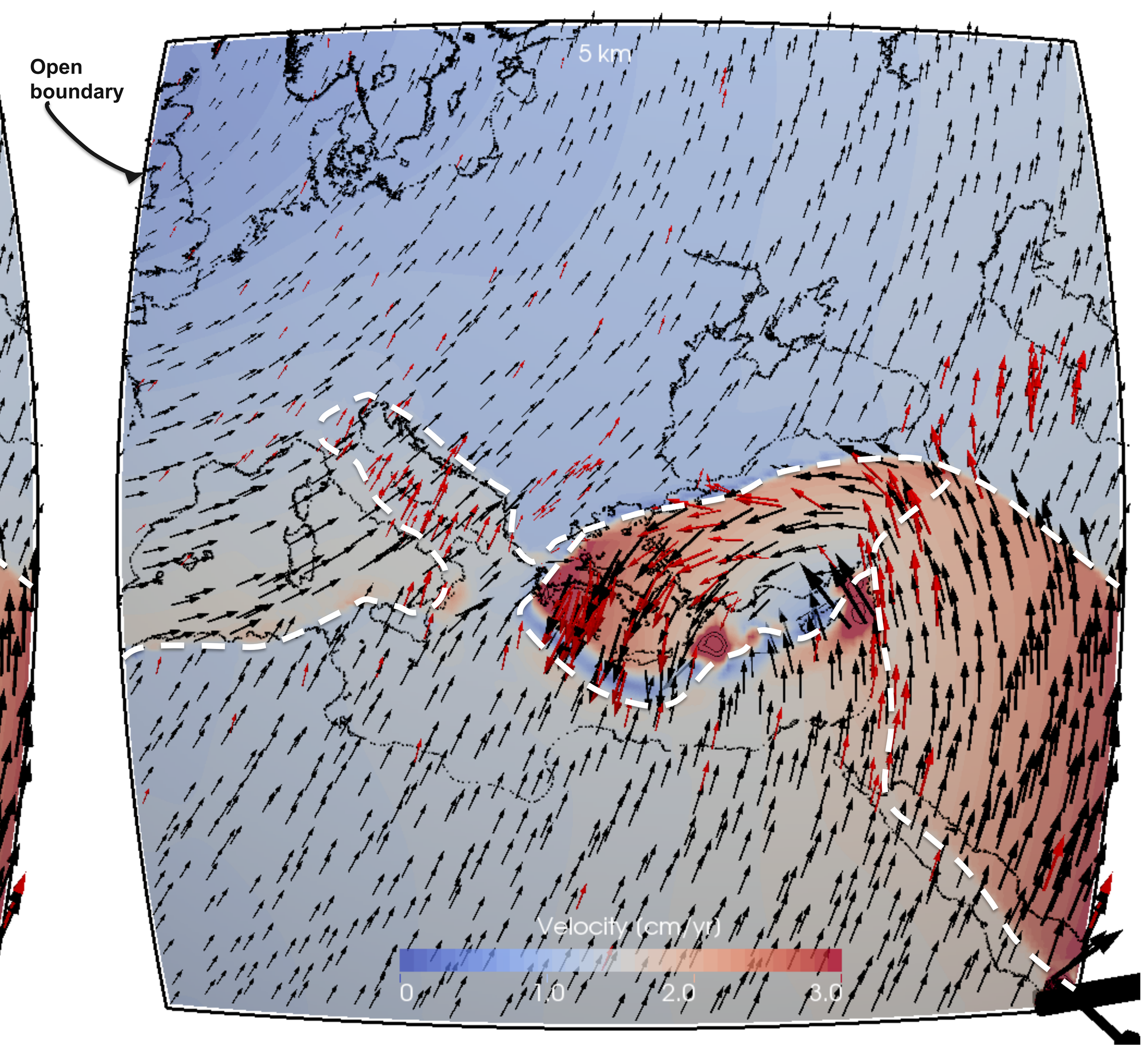

Figure 6 When leaving the western domain boundary completely open (so not prescribing plate motions), lithospheric inflow through this boundary is more eastward. Also, Eurasia motion in the Western Mediterranean region is faster. Motion of the Aegean plate is reduced, resulting in a better match GPS velocity magnitudes.

References

Amaru, M. L., 2007. Global travel time tomography with 3-D reference models.
Carafa, M. M. C. et al. 2015. Journal of Geophysical Research: Solid Earth, 120.
Chertova, M. V. et al. 2012. Solid Earth, 3, 313-326.
Connolly, J. A. D., 2009. Geophysical Research Letters, 10, Q10014.
Doubrovine, P.V. et al. 2012. Journal of Geophysical Research, 117, B09101.
Faccenna, C. et al. 2014. Reviews of Geophysics, 52.
Kronbichler, M. et al. , 2012. Geophysical Journal International, 191, 12-29.
Lu, C. and Grand, S. P., 2016. Geophysical Journal International, 205, 1074-1085.
NCEDC, 2014. Northern California Earthquake Data Center, UC Berkeley Seismological Laboratory. Dataset.
Nocquet, J.-M., 2012. Tectonophysics, 579, 220-242.
Steinberger, B. and Calderwood, A.R., 2006. Geophysical Journal International, 167, 3, 1471-1481.
Van Hinsbergen, D. J. J. et al. 2005. Geology, 33, 325-328.